

Microstructure evolution in Zr-Mo multilayers induced by ion irradiation

This article has been downloaded from IOPscience. Please scroll down to see the full text article.

1995 J. Phys.: Condens. Matter 7 2667

(<http://iopscience.iop.org/0953-8984/7/14/007>)

View [the table of contents for this issue](#), or go to the [journal homepage](#) for more

Download details:

IP Address: 171.66.16.179

The article was downloaded on 13/05/2010 at 12:52

Please note that [terms and conditions apply](#).

Microstructure evolution in Zr–Mo multilayers induced by ion irradiation

O Jin† and B X Liu†‡

† Department of Materials Science and Engineering, Tsinghua University, Beijing 100084, People's Republic of China

‡ Center of Condensed Matter and Radiation Physics, China Center of Advanced Science and Technology (World Laboratory), Beijing 100080, People's Republic of China

Received 5 October 1994

Abstract. Amorphization was achieved by room-temperature 200 keV xenon ion mixing in Zr–Mo multilayered films. In addition, two new Mo-based metastable crystalline phases were obtained, which were of FCC and HCP structures, respectively. A Gibbs free-energy diagram that concerns the free-energy curves of the amorphous phase and the terminal solid solutions was constructed to give related thermodynamic explanations to the observations.

Accompanied by the exploration of various new materials, amorphous alloys have long been attractive, because they are expected to have many novel properties. Since the amorphous state is not an equilibrium state, new techniques are needed to produce new amorphous materials and they naturally stimulate the progress of the theory of alloys under the non-equilibrium process. Ion beam mixing of multilayered films has flourished since the 1980s and proved to be a powerful means of producing metastable alloys of amorphous as well as metastable crystalline (MX) structures [1, 2]. Meanwhile, as ion mixing is a process far from equilibrium and it is possible to trace the phase evolution experimentally by increasing the irradiation dose stepwise, it has been employed to reveal the intrinsic mechanism of the metastable phase formation.

To date, a great number of new metastable alloys have been obtained by ion mixing in some 70 metal systems and, among them, some new alloys have not been obtained by other equilibrium and non-equilibrium techniques [3–5]. Although it is not understood on an atomic scale owing to the complexity of the non-equilibrium process, some empirical models have been proposed on the basis of the static properties of the components and the features of the equilibrium phase diagram, which generally focused on the glass-forming ability of the binary metal systems [6–8].

Recently, the MX phase formation has been paid more attention because of some new revelations. At the same time, respective explanations in terms of thermodynamics and growth kinetics have been suggested [9, 10].

In the present paper, we report the phase changes upon ion mixing in Zr–Mo multilayers, and the formation of amorphous and two new MX phases. To interpret the observations in this binary metal system, a free-energy diagram was constructed on the basis of the model of Miedema *et al* [11] and the method proposed by Alonso *et al* [12].

Zr–Mo multilayered samples were prepared by depositing alternately pure zirconium (99.9%) and pure molybdenum (99.9%) onto NaCl single-crystal substrates in an electron gun evaporation system with a vacuum level of the order of 10^{-5} Pa. The total thickness of

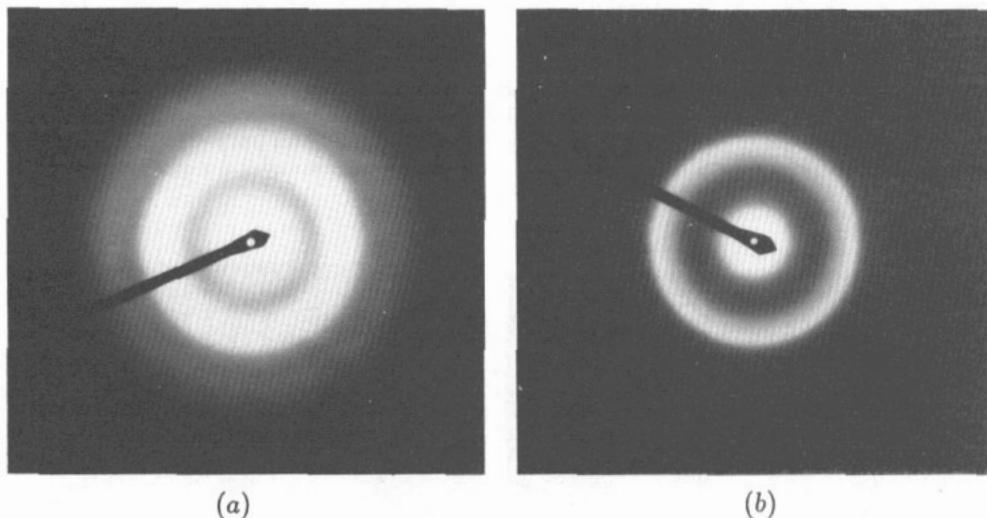
the films was about 50 nm, which approximately corresponded to the projected range plus projected range straggling of the irradiation ions, i.e. 200 keV xenon ions. The number of layers for each sample was nine to ten and the thickness of each layer varied according to the designed composition. As-deposited films were then irradiated at room temperature with 200 keV xenon ions to doses of 3×10^{14} – 1×10^{16} Xe^+ cm^{-2} . The vacuum level during irradiation was better than 5×10^{-4} Pa and the ion current density was less than $1 \mu\text{A cm}^{-2}$ to avoid overheating. All samples were investigated by transmission electron microscopy (TEM) observations and selected-area diffraction (SAD) to identify the structure of the resultant phases. Energy-dispersive spectroscopy analysis was employed to determine the average composition of the as-deposited films, as well as the real compositions of the resultant phases in the irradiated samples with an experimental error of 5%.

Table 1 lists the phase changes in the Zr–Mo multilayered films under room-temperature 200 keV xenon ion irradiation. One sees that, in both the $\text{Zr}_{46}\text{Mo}_{54}$ and the $\text{Zr}_{75}\text{Mo}_{25}$ samples, amorphous phases were formed at a dose of 7×10^{14} Xe^+ cm^{-2} . Also, amorphization was achieved in the $\text{Zr}_{80}\text{Mo}_{20}$ sample at a dose of 1×10^{15} Xe^+ cm^{-2} . From these it is suggested that the amorphization range in the Zr–Mo system can at least extend from $\text{Zr}_{46}\text{Mo}_{54}$ to $\text{Zr}_{80}\text{Mo}_{20}$. The recrystallization temperature of the ion-mixed amorphous phases was around 700°C determined by TEM *in-situ* annealing. By careful TEM examination, some difference between the microstructures of the amorphous phases formed in different samples was observed. Figure 1 shows two SAD patterns of the amorphous phases. One sees that the amorphous halo in the $\text{Zr}_{75}\text{Mo}_{25}$ sample is located as usual somewhere in between the Zr(100) and the Mo(110), as shown in figure 1(a), while figure 1(b) shows that the inner halo of the $\text{Zr}_{46}\text{Mo}_{54}$ amorphous phase is divided into two separate haloes, corresponding to the Zr(100) and the Mo(110) diffraction lines, respectively. This suggests that there exist two different disordered atom clusters in the $\text{Zr}_{46}\text{Mo}_{54}$ sample, i.e. one is Zr rich and the other is Mo rich. Interestingly, as shown in figure 2, when the irradiation dose is increased to 7×10^{15} Xe^+ cm^{-2} , a MX phase of FCC structure was formed and its (111) line is situated at the halo related to Mo while the other halo still remains. As for the $\text{Zr}_{75}\text{Mo}_{25}$ sample, the amorphous phase evolved into two coexistent phases at a dose of 5×10^{15} Xe^+ cm^{-2} , i.e. a hexagonal phase and an amorphous phase differing in the halo position from the previous one as evidenced by the SAD pattern in figure 3. The lattice parameters of the formed hexagonal phase were $a = 2.97 \text{ \AA}$, $c = 4.75 \text{ \AA}$ and $c/a = 1.60$, which were close to those of the pure zirconium. These experimental observations suggested that the previously formed amorphous phase transformed into a Zr-based solid solution and an amorphous phase certainly of Mo enriched at the higher dose. When the irradiation dose was increased further to 7×10^{15} Xe^+ cm^{-2} , amorphization was achieved again.

In the $\text{Zr}_7\text{Mo}_{93}$ sample, when the irradiation dose 5×10^{15} Xe^+ cm^{-2} , the BCC Mo-based solid solution transformed into a new MX phase of FCC structure, as shown in figure 4. Upon further irradiation to a dose of 1×10^{16} Xe^+ cm^{-2} , a HCP phase emerged with a few diffraction lines of the FCC phase still remaining. Figure 5 shows the SAD patterns of these phases and tables 2 and 3 list the indexing results of the two MX phases. It is unusual to have observed these MX phases of FCC and HCP structures at a composition very close to pure molybdenum of BCC structure. To find the possible crystallographic correlation, the lattice constant of the FCC structure evolved from pure molybdenum was deduced to be 3.97 \AA , if applying the model of constant atomic volume. The calculated constant is a little smaller than that of the observed constant for the $\text{Zr}_7\text{Mo}_{93}$ sample, which probably resulted from dissolving some Zr atoms into the molybdenum. A similar FCC phase with a lattice parameter of 4.19 \AA was also observed for the $\text{Zr}_{46}\text{Mo}_{54}$ sample at a dose of 7×10^{15} Xe^+ cm^{-2} .

Table 1. Phase evolution of the Zr-Mo multilayered films upon room-temperature 200 keV xenon ion mixing. —, no data obtained.

	Phase at the following dose			
	$7 \times 10^{14} \text{ Xe}^+ \text{ cm}^{-2}$	$5 \times 10^{15} \text{ Xe}^+ \text{ cm}^{-2}$	$7 \times 10^{15} \text{ Xe}^+ \text{ cm}^{-2}$	$1 \times 10^{16} \text{ Xe}^+ \text{ cm}^{-2}$
Zr ₇ Mo ₉₃	BCC, $a = 2.96 \text{ \AA}$	FCC, $a = 4.31 \text{ \AA}$	—	HCP, $a = 2.91 \text{ \AA}$, $c/a = 1.59$ FCC, $a = 4.31 \text{ \AA}$
Zr ₄₆ Mo ₅₄	Amorphous	Amorphous	FCC $a = 4.19 \text{ \AA}$ Amorphous	—
Zr ₇₅ Mo ₂₅	Amorphous	HCP $a = 2.97 \text{ \AA}$, $c/a = 1.60$ Amorphous		

**Figure 1.** SAD patterns of the amorphous phases formed in the (a) Zr₇₅Mo₂₅ and (b) Zr₄₆Mo₅₄ multilayered samples by room-temperature 200 keV xenon ion mixing at a dose of $7 \times 10^{14} \text{ Xe}^+ \text{ cm}^{-2}$.

Usually the Gibbs free energy can serve as a criterion for comparing the relative thermal stability of the possible states in the systems and can be expressed as $\Delta G = \Delta H - T\Delta S$, where ΔH and ΔS are the enthalpy of formation and the entropy of formation, respectively. The entropy of formation can be taken, as a first approximation, as that of an ideal solid solution, i.e. $\Delta S = -R(X_A \ln X_A + X_B \ln X_B)$, where R is the gas constant, and X_A and X_B are the atomic concentration of metals A and B in the alloy, respectively. The enthalpy of formation, which plays an important role in the theory of Miedema *et al.*, of a substitutional solid solution of transition metals is the sum of three terms [13–15]:

$$\Delta H = \Delta H^c + \Delta H^e + \Delta H^s \quad (1)$$

where ΔH^c , ΔH^e and ΔH^s are regarded as the chemical contribution, the elastic or size-mismatch contribution and the structural contribution, respectively.

Specifically, for an amorphous phase both the elastic and the structural terms are absent. Following the suggestion by Niessen *et al.* [16], the enthalpy of the amorphous phase is

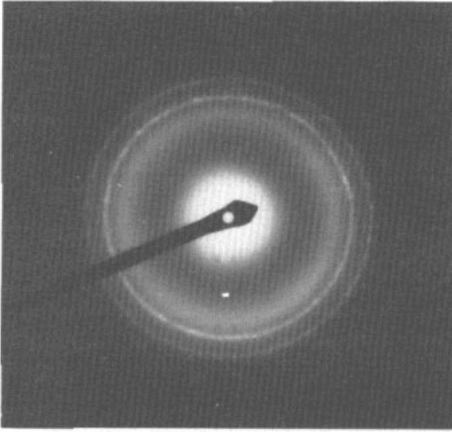


Figure 2. SAD pattern of the coexistent FCC and amorphous phases formed in the $Zr_{46}Mo_{54}$ multilayered sample by room-temperature 200 keV xenon ion mixing at a dose of $7 \times 10^{15} \text{ Xe}^+ \text{ cm}^{-2}$.

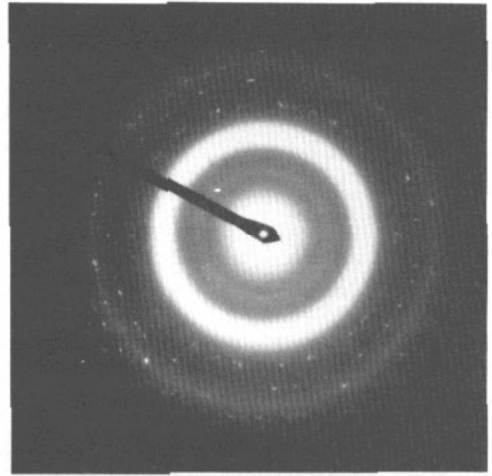


Figure 3. SAD pattern of the coexistent HCP-Zr-based solid solution and amorphous phases formed in the $Zr_{75}Mo_{25}$ multilayered sample by room-temperature 200 keV xenon ion mixing at a dose of $5 \times 10^{15} \text{ Xe}^+ \text{ cm}^{-2}$.

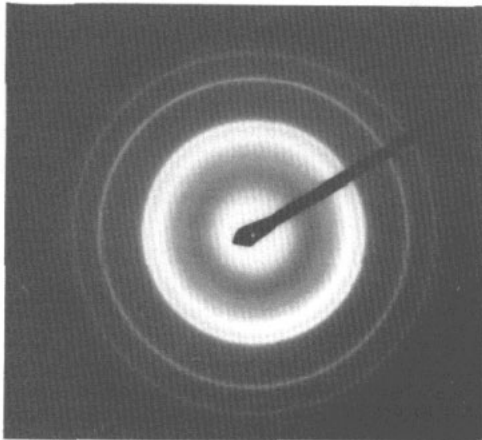


Figure 4. SAD pattern of the FCC phase formed in the Zr_7Mo_{93} multilayered sample by room-temperature 200 keV xenon ion mixing at a dose of $5 \times 10^{15} \text{ Xe}^+ \text{ cm}^{-2}$.

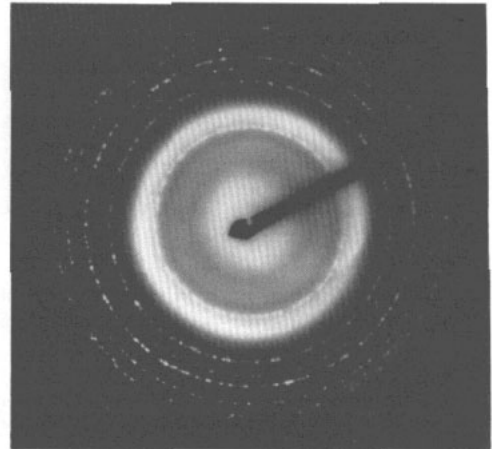


Figure 5. SAD pattern of the coexistent HCP and FCC phases formed in the Zr_7Mo_{93} multilayered sample by room-temperature 200 keV xenon ion mixing at a dose of $1 \times 10^{16} \text{ Xe}^+ \text{ cm}^{-2}$.

given by

$$\Delta H_{\text{amorphous}} = \Delta H^c + \alpha(X_A T_{m,A} + X_B T_{m,B}) \quad (2)$$

where α is an empirical constant equal to $3.5 \text{ J mol}^{-1} \text{ K}^{-1}$ and $T_{m,i}$ is the melting point of the component i , i.e. 2125 K for Zr and 2883 K for Mo.

The Gibbs free-energy curves of the amorphous phase and two terminal solid solutions were calculated by the method discussed above and are shown in figure 6. One can see

Table 2. The indexing results of the MX phase of FCC structure formed in the Zr₇Mo₉₃ sample by 200 keV xenon ion mixing at a dose of 5×10^{15} Xe⁺ cm⁻². The lattice parameter $a = 4.31$ Å.

d_{exp} (Å)	Intensity	hkl	d_{calc} (Å)
2.49	Strong	111	2.49
2.15	Strong	200	2.16
1.53	Medium	220	1.52
1.31	Medium	311	1.30
1.25	Weak	222	1.24
1.08	Weak	400	1.08
0.99	Weak	331	0.99
0.97	Weak	420	0.96
0.88	Weak	422	0.88
0.83	Weak	333, 511	0.83
0.76	Weak	440	0.76
0.72	Weak	442	0.72

Table 3. The indexing results of the MX phase of HCP structure formed in the Zr₇Mo₉₃ sample by 200 keV xenon ion mixing at a dose of 1×10^{16} Xe⁺ cm⁻². The lattice parameter $a = 2.91$ Å; $c/a = 1.59$.

d_{exp} (Å)	Intensity	hkl	d_{calc} (Å)
2.52	Strong	100	2.52
2.32	Strong	002	2.32
2.21	Strong	101	2.22
1.71	Medium	102	1.71
1.53	Medium	220 ^a	1.52
1.44	Medium	110	1.46
1.30	Medium	103, 311 ^a	1.32
1.25	Medium	200, 222 ^a	1.26
1.21	Medium	112, 201	1.22
1.14	Weak	004	1.16
1.09	Weak	202	1.11
1.04	Weak	104	1.05
0.96	Weak	203	0.98
0.94	Weak	211	0.93
0.92	Weak	114	0.91

^a Data belonging to the FCC MX phase which is the same as formed at a dose of 5×10^{15} Xe⁺ cm⁻².

from the figure that from the Mo concentration about 12 to 65 at.% the free-energy curve of amorphous phase was below that of the two solid solutions. This means that, between these concentrations, amorphization was favoured in the system, which is in agreement with the ion-mixing results mentioned above. It is of interest to note that the energy state of the Zr₇₅Mo₂₅ sample can also be situated on the common tangent of the Zr-based solid solution and the amorphous phase. In this case, these two phases would coexist simultaneously, and this was indeed observed in the ion-mixed sample at a dose of 5×10^{15} Xe⁺ cm⁻². The calculation of the free energy for the MX phases is still under investigation.

Acknowledgments

The authors are grateful to the researchers of the Transmission Electron Microscopy Laboratory of Peking University and the Analysis Center of Tsinghua University for their

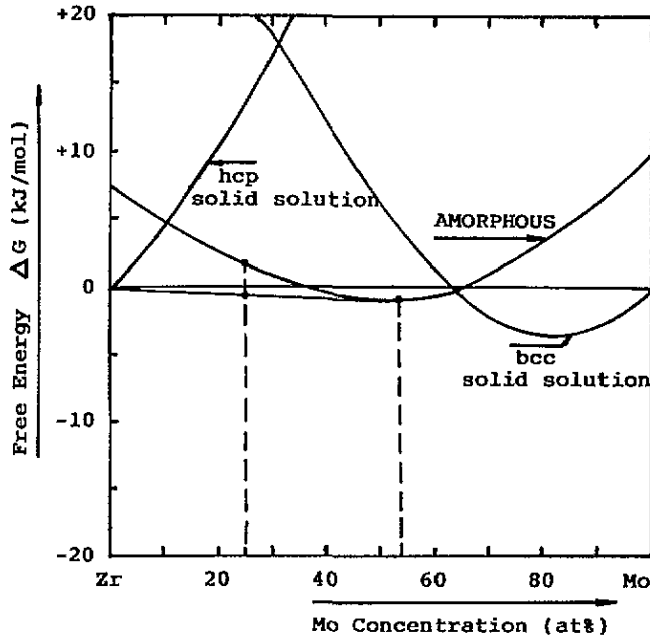


Figure 6. Calculated Gibbs free-energy diagram of the Zr-Mo system.

help. Financial support from the National Natural Science Foundation of China and funding support from Tsinghua University is also appreciated.

References

- [1] Liu B X 1986 *Phys. Status Solidi* a 94 11
- [2] Blatter A and Allmen M V 1985 *Phys. Rev. Lett.* 54 2103
- [3] Liu B X, Che D Z, Zhang Z J, Lai S L and Ding J R 1991 *Phys. Status Solidi* a 128 345
- [4] Liu B X and Nicolet M A 1983 *Thin Solid Films* 101 201
- [5] Jin O and Liu B X 1994 *J. Phys.: Condens. Matter* 6 L39
- [6] Alonso J A and Simozar S 1983 *Solid State Commun.* 48 765
- [7] Liu B X, Johnson W L, Nicolet M-A and Lau S S 1983 *Appl. Phys. Lett.* 42 45
- [8] Ossi P M 1990 *Phys. Status Solidi* a 119 463
- [9] Zhang Z J, Bai H Y, Qiu Q L, Yang T, Tao K and Liu B X 1993 *J. Appl. Phys.* 73 1702
- [10] Zhang Z J and Liu B X 1994 *J. Phys.: Condens. Matter* 6 2647
- [11] Miedema A R, Niessen A K, deBoer F R, Boom R and Mattens W C M 1989 *Cohesion in Metals: Transition Metal Alloys* (Amsterdam: North-Holland)
- [12] Alonso J A, Gallego L J and Simozar J A 1990 *Nuovo Cimento* 12 587
- [13] Niessen A K and Miedema A R 1983 *Ber. Bunsenges. Phys. Chem.* 87 717
- [14] Lopez J M and Alonso J A 1985 *Z. Naturforsch.* a 40 1199
- [15] Weeber A W 1987 *J. Phys. F: Met. Phys.* 17 809
- [16] Niessen A K, Miedema A R, deBoer F R and Boom R 1988 *Physica* B 151 401